



HAL
open science

Effect of inter-ply sliding on the quality of multilayer interlock dry fabric preforms

Samir Allaoui, Christophe Cellard, G. Hivet

► **To cite this version:**

Samir Allaoui, Christophe Cellard, G. Hivet. Effect of inter-ply sliding on the quality of multilayer interlock dry fabric preforms. *Composites Part A: Applied Science and Manufacturing*, 2015, 68, pp.336-345. 10.1016/j.compositesa.2014.10.017. hal-01091693

HAL Id: hal-01091693

<https://hal.science/hal-01091693>

Submitted on 10 Apr 2018

HAL is a multi-disciplinary open access archive for the deposit and dissemination of scientific research documents, whether they are published or not. The documents may come from teaching and research institutions in France or abroad, or from public or private research centers.

L'archive ouverte pluridisciplinaire **HAL**, est destinée au dépôt et à la diffusion de documents scientifiques de niveau recherche, publiés ou non, émanant des établissements d'enseignement et de recherche français ou étrangers, des laboratoires publics ou privés.

Effect of inter-ply sliding on the quality of multilayer interlock dry fabric preforms

S. Allaoui^{a*}, C. Cellard^b, G. Hivet^a

^a Univ. Orléans, PRISME, EA 4229, F45072, Orléans, France.

^b University of Brest, EA 4325 LBMS, 6 Avenue Victor Le Gorgeu – CS 93837, 29238 Brest Cedex 3, France

* Corresponding author (samir.allaoui@univ-orleans.fr)

Keywords: E. Forming; B. Defects; A. Fabrics/textiles; A. Lamina/ply.

Abstract

Forming thick, complex shapes with several layers is needed in high technology fields. During forming, defects can occur and have to be taken into account because they can significantly affect the mechanical performance of the part. This experimental study shows that, when working with dry fabric forming, the type and number of defects is a function of the punch geometry, the process parameters, the orientation of the fabric with respect to the punch and the inter-ply friction. Inter-ply friction has a huge effect on the quality of the preform when inter-ply sliding occurs. This inter-ply Friction leads to several overhanging yarn shocks that generate high tangential forces, which inhibit the relative sliding of plies. In addition, to reduce the number and amplitude of defects, the layers subjected to severe defects can be placed in the inner position where they are subjected to the compression applied by the upper layers.

1. Introduction

Global trends towards CO₂ reduction in the transportation sector and resource efficiency have significantly increased the importance of the use of materials that are lightweight, while still maintaining structural performance. Designing and manufacturing viable lightweight vehicles for automotive and aeronautic transportation can be achieved by replacing metallic materials with composites on structural parts with equal mechanical performances. As a result of their good strength/weight ratio and their anisotropy which can be adapted to the mechanical loading of the structure, composite materials are a suitable solution to the optimization of large thick structural parts with complex geometries.

To manufacture complex composite parts and structures, Liquid Composite Molding (LCM) processes are among the best candidates because they offer a good compromise in terms of repeatability, production rates, low-energy consumption and low final cost. The first step of these processes consists of draping a dry preform before the liquid resin is injected. This preforming is a challenging phase, and the physical mechanisms are complex and far from being fully understood [1]. Lack of understanding of these mechanisms hampers the control of the manufacturing process and the development of composite

materials. In addition, the increasing use of materials with low environmental effects (Biomaterials) and complex weaving architectures (interlock, 3D fabrics) makes this process more difficult.

Among all the strategies available to investigate the formability of a given fabric on a given shape, finite element simulations and experimental demonstrators can be considered. The complementarity features between these two methods make it possible to understand and to model accurately the preforming step and will hopefully decrease the cost and time needed for the development of tools and fabrics. Many methods have been proposed recently to achieve sheet forming simulations of dry fabrics (e.g. [2-4]). These studies need several parameters such as dry fabric mechanical properties and fabric/tool friction coefficient, which have been widely studied [5-10]. The results obtained must be validated with data of woven reinforcement forming using experimental approaches [11-14].

When working with multilayer forming of thick composite parts, inter-ply sliding can occur. This sliding generates inter-ply friction. Several numerical studies (some of them correlated with experimental results) have highlighted this effect during the forming of pre-consolidated laminated composites [15-19]. Ten Thije and Akkerman showed that the behavior of the layered composites heavily depends on the fold's stacking sequences [15]. They conducted forming experiments of pre-consolidated four-layer satin weave PPS (polyphenylene sulfide) laminates on a dome geometry and demonstrated that the number and size of wrinkles increased as the offset in the lay-up angle increased. The occurrence of wrinkling was attributed to the fact that, for a large offset in the lay-up, inter-ply slipping is blocked by the fibers of the other plies resulting in load transfers between individual plies [15]. However, the laminates were loosely clamped during forming while it is known that layer behavior, and thus wrinkling, is highly dependent on the tension, friction and boundary conditions [20-22]. Indeed, forming tests under tension of pre-consolidated sheets conducted by Harrison et al. on the double-dome benchmark geometry produced no wrinkles and no inter-ply sliding [16]. Nevertheless, the study by Bel et al. done on one layer of dry NCF (non-crimp fabric), which was subjected to higher frictional forces, on the same kind of shape revealed some slippage between the two yarn networks [23]. This difference is not explained by Harrison et al. in their paper which states that forming multiple layers of yarns is not well understood at the moment.

For the multilayered forming of dry fabric only numerical studies are available. They have shown that inter-ply friction is a key point for the quality of the final shape [24-26]. These studies were conducted on simple geometries (such as hemisphere) on which few or no defects occur whereas it has been shown that the occurrence of defects, and thus fabric formability on a given punch, depends on the punch geometry and especially its curvatures [27]. Some studies were also conducted on nonwoven reinforcement (NCF) [23,24]. The effect of the inter-ply friction with this kind of fabric is less severe than with woven fabrics because phenomena such as shocks between overhanging yarns [28, 29] do not occur. The shocks consist of frontal contact between yarns that leads to an increase in reaction forces during sliding. Therefore, the use of woven fabric reinforcement leads to the occurrence or amplification of defects. There are no experimental studies investigating the effect of friction on the multilayered preforming of dry woven reinforcement on complex and deep shapes that lead to high shear angles (up to

60°) and various defects [12,27]. The knowledge and understanding of the effect of friction on the behavior of the preform is, however, necessary to control the processes.

The aim of this study is therefore to investigate experimentally the effect of fabric/fabric friction on the occurrence of defects in multilayered highly double curved shaping of interlock dry woven fabric. For this purpose, forming tests using an interlock fabric were conducted and the results obtained on single-layer and multilayer formings were compared with a focus on the shear angle values and the defects quantification.

2. Material and method

2.1. Tested Fabric

The tests presented in this paper were completed on a commercial composite woven reinforcement used in the aeronautic field. It is a powdered interlock fabric, denoted Hexcel G1151[®] with an areal weight of 630 g/m². It is composed of T300JB 6K carbon yarns. Three weft yarn layers are linked by the weaving. The unit cell consists of six warp yarns and 15 weft yarns with a nominal construction of 7.5 yarns/cm for warp and 7.4 yarns/cm for weft. The yarn widths are approximately 2 mm for warp and 3 mm for weft. The mechanical behavior of this fabric has been widely studied [5-7, 29].

2.2. Forming device

An experimental device developed in collaboration with the EADS Company was used to conduct the preforming tests [11, 27]. It is composed of three parts. The first part consists of a punch/open-die set that can be easily changed. The punch is moved using an electric jack to control the punch position and speed. The die is open to allow for optical measurement on the fabric during stamping using the second part of the device composed of a stereo vision system. The latter consists of two commercial Charge Coupled Device (CCD) cameras connected to a computer allowing the continuous recording of images of the samples during the shaping process. Digital images can be post-processed to calculate the displacement and strain fields using software based on Digital Image Correlation (DIC) or marker tracking techniques. The third part of the device is a pre-tensioning system composed of independent blank-holders actuated by pneumatic jacks. The number and geometry of the blank-holders can be easily changed to investigate their influence on the shape quality.

2.3. Test conditions

There is a complex relationship among the fabric mechanical properties, the forming process parameters (e.g. blank-holder pressure distribution, ...) and the shape of the part. Because our study concerns the effect of inter-ply sliding on the occurrence of defects, test conditions and shapes that will admit the occurrence of defects must be chosen.

The first important point is the choice of a highly double-curved and deep-draw shape that can generate a wide range of defects with significant amplitudes. While experimental data on multilayer forming can be found in the literature, the tests were performed on simple and shallow shapes such as a hemisphere [15, 24, 25] or a double-dome [16] which do not promote the occurrence of defects. For this reason, a prismatic punch with triple points, that is highly non-expandable with small curvature radii (10

mm), used previously for forming a corner case was chosen for this study (Figure 1). The dimensions of the punch can be found on Figure 1. The height of the final preform obtained with this punch is approximately 175 mm while those obtained with the dome or double-dome geometries have a maximum depth of 100 mm [15,16,23-26].

The second point concerns the process parameters which must be chosen in accordance with the fabric behavior. To form complex shapes such as the one concerned in this study, the fabric may need to accommodate large in-plane shear deformation. It was shown that the G1151[®] fabric is particularly well-adapted to this deformation mode, with a high locking angle (~55–60°) [5-7]. When the shear angle comes close to the “locking angle”, the shear stiffness increases and the fabric may start wrinkling. This is one of the most well-known forming defects that has to be avoided because it results in a significant decrease in the mechanical properties of the cured composite part.

A wrinkle is an out-of-plane phenomenon that occurs when less energy is needed for an out-of-plane deformation than for an in-plane deformation. The notion of a locking angle is therefore not necessarily sufficient to anticipate the presence of wrinkles, because wrinkling (position, shape, number...) is strongly related not only to the bending stiffness but also to the tensile loading on the woven fabric [22, 27]. Coupling between shear and tension is an effect related to the woven fabric and has been discussed in different papers showing a delay in the onset of wrinkles during shear tests with pretension [5, 30, 31]. Thus, it is possible to obtain a higher shear deformation, than could be expected if only considering the locking angle, when tension is applied to the fabric. As a result, an increase in the tension applied on the interlock fabric tends to delay the onset of wrinkles [27].

However, increasing the tension applied on the yarns can lead to significant residual stresses in the fabric. The consistency of the reinforcement may then be undermined, thereby resulting in other defects such as broken yarns and/or the "weave pattern heterogeneity" phenomenon [27]. These defect zones are more extended than that of the wrinkles and the induced frictional forces are significant. Thus, forming with a high blank-holder pressure was chosen for this study to ensure maximum defects on the final parts. Based on the previously discussed influences, forming tests were conducted with eight blank-holders around the preform to apply tension on the yarns through fabric/metal friction (Figure 2). An effective pressure on the fabric of 0.1 bar was applied by the blank-holders which corresponds to an applied force of 9.22 N/yarn when forming one layer.

These test conditions were applied for monolayer and two-layered forming of the prismatic shape for two configurations. In the first one, the fabric was initially positioned with the weft and warp networks parallel to the edges of the punch faces (Figure 2). This configuration was performed with a rotation angle equal to zero ($\alpha=0^\circ$) and was considered as the reference. To assess the inter-ply friction effect, forming tests were conducted with one and two layers, which were superimposed with the same orientation. Qualitative and quantitative comparisons were then made between the two shapes obtained. To demonstrate that the influence of fabric/fabric friction strongly depends on the relative orientation of the layers, a two-ply forming by varying a relative angle α was chosen for the second configuration. One layer was kept at the reference orientation ($\alpha=0^\circ$) and the other one was rotated with angles of 30°, 45° and 60° (Figure 2). As for the reference configuration, monolayer forming tests were performed at the

same orientations to evaluate the inter-ply friction effect. To make the comparison as consistent as possible, the two-ply forming tests were done by putting the rotated layer in the lower position (Figure 2). Consequently, the presence of the upper layer, and thus the compaction exerted by the latter and by the inter-ply friction, is the only difference between the monolayer and multilayer forming. However, the preform must be demolded to see the oriented layers, to observe the defects and make measurements. For that purpose, the preform was fixed by melting the powdered resin on the fabric using a heater. Once the resin had hardened, the preform was gently removed to avoid modifying the preform state. This step is tricky and can introduce variations in the amplitude of defects. To assess the potential impact, two-layer preforming was also performed by putting the oriented ply on the top of the preform. The results of the two positions were compared.

To distinguish among the different configurations of two-ply forming, the following notation will be adopted: X°/Y° where the first angle (X°) represents the orientation of the upper ply and the second one (Y°) the orientation angle of the lower ply.

For each configuration three forming tests were done. The punch speed was 30 mm/min, which is in the range of what is currently requested by our industrial partners for forming studies. Defects and shear angles were quantified. Quantitative and qualitative comparisons were made among the different configurations. Moreover, to measure the sliding distance between plies when forming two layers, markers were painted on the two folds at the same locations. The markers were placed on half of the preform (to cover a symmetrical part) along lines to cover all the representative areas (lines A to G on Figure 2). The plies were positioned carefully so as to match each pair of points. After the shape had been frozen and demolded, the displacement of each pair of points was measured.

3. Results and discussion

3.1. Reference configuration

The forming tests in configuration 1 with a rotation angle $\alpha=0^\circ$ give a good shape quality at the macroscopic level as depicted in figure 3. An outside view of the preforms, realized with one and two layers (0° and $0^\circ/0^\circ$), shows that the agreement with the punch shape at the end of the forming is fairly good (Figure 3). Wrinkles occur as was foreseen but not in the “useful zone”. The useful zone contains the final part surfaces, that is to say, the areas remaining after the excess fabric has been cut away. In the current study, it consists of the prismatic preform areas (Figure 3). Thus, these wrinkles have no effect on the quality of the final part because the zones on which they appear are cut away after forming. Previous tests with a lower blank-holder pressure in the same configuration led to wrinkles on the useful areas [27]. These results, therefore, confirm the influence of tension in yarns, due to the blank-holder pressure, on the presence of wrinkles.

Another type of defect: “out-of-plane buckles” occur on the faces and edges of the prismatic preforms (Figure 3 and Figure 4). Fabric wrinkling and yarn buckling are very different phenomena. While both are a form of buckling, the result and scale in the two cases are different. Wrinkling is a fabric-scale strain mode resulting in a classical membrane out-of-plane bending; the fabric structure and architecture are not impacted. This strain mode is exactly the same as if the fabric was a continuous

material. It can be compared, for instance to the wrinkling of a sheet of steel. A “buckle, on the other hand, is a meso-scale (yarn scale) phenomenon that only concerns individual yarns and does not result in any membrane strain. Only the fabric architecture and structure are impacted, because one (or several) yarns, are submitted to out-of-plane bending, go outside of the fabric, and hence no longer respect the weaving pattern. [27]. This second defect only results from the heterogeneous nature of fabrics. In sum, a wrinkle is a global membrane defect, whereas a buckle is a local irregularity.

Buckles are expected to occur along the yarns (of each network) passing through the triple points because the shearing of the fabric on each side of these yarns is in two opposite directions (clockwise on one side and counterclockwise on the other). This shearing leads to in-plane bending of yarns as shown on Figure 4 by the red line. Locally, these buckles constitute a finite overthickness and fiber disorientation that leads to a local heterogeneity of the fabric. For the prismatic shapes manufactured according to configuration 1, buckles are located at the middle of the triangular faces and on the diagonal edges separating the triangular from the rectangular faces, on areas of approximately 15 to 35 mm in width (Figure 4). The location and magnitudes of the wrinkles and buckles are almost the same for single-ply and multiply formings.

Figure 4 shows the measured shear angles on the front face (triangular one) of the two-ply shape where the highest shear angles were measured on the fabric. The angles vary between 46° and 50° in the upper layer and between 45° and 49° in the inner one while the measured angles for the single-ply shape are approximately $49 \pm 1^\circ$. The shear angles remain approximately the same between the single-ply and the two-ply shapes. In addition, the highest shear angles were achieved in the bottom corners (up to 55°) but without creating wrinkles. In conclusion, the magnitude of the defects, the areas in which they occur as well as the shear angles of the fabric on the outer faces are approximately the same for the single-ply and multiply forming when the layers are oriented at 0° . This fact was confirmed on multilayer preforming tests done with four layers. This difference can be explained by the low inter-ply sliding that will be discussed in more detail in section 3.3.

A different conclusion is reached when considering defects that occur on the inner faces. In fact, additional defects can be observed and a difference between the single-layer and multilayer forming can be observed. The “out-of-plane buckles” occur in the same areas and with the same magnitude on the inner and outer faces of the single-ply and two-ply shapes (Figure 5 detail a). However, additional defects such as broken fibers, buckles and wrinkles occur on some areas of the inner faces whereas they were not observed on the outer faces. Fiber breakage was observed on the prismatic shape's triple points but with a larger extent in the case of the multilayer shape (Figure 5 detail b). This fiber damage is more likely due to the severe stresses generated by the boundary conditions (small curvature radii of the triple point) and the pressure exerted by the upper layer on the lower one. These conditions, associated to the ply/ply friction, are also the cause of the buckles and the “weave pattern heterogeneity” that were observed on the bottom corners of the inner faces (Figure 5 detail c). “Weave pattern heterogeneity” is caused by a relative slip of the weft and warp yarns and leads to a very low local yarn density [27]. These defects were only observed on the inner faces of the shape formed with two interlock layers. They mainly depend on the complexity of the shape, the boundary conditions and the cohesion of the fabric weaving. On the

inner layers, wrinkles were observed for the multilayer shape (Figure 5 detail d). The presence of this defect in this area may appear surprising because of the high blank-holder pressure and the small shear angles reached at these faces ($<10^\circ$). However, it can be explained by the springback occurring after the heating (to fix) and demolding of the preform.

3.2. Oriented layers configuration

3.2.1. Monolayer forming: α°

The monolayer shapes produced with configuration 2 showed more extensive defects (Figure 6) than with configuration 1. Note that there is symmetry, i.e. the faces not shown on this figure exhibit the same defects as the opposite ones. The external view of the single-layer shape (45°) shows wrinkles and “weave pattern heterogeneity” in addition to “out-of-plane buckles” (Figure 6.a). The buckles are located on the front faces, the bottom corners and the side faces (Figure 6.a). The buckle positions are therefore different from the single-layer shape obtained according to the reference configuration (0°) and are more numerous. This difference is assumed to be due to the relative position between the fabric and the punch.

In addition other defects occur in this configuration. These defects are the “weave pattern heterogeneity”, associated with the buckles, which occur in the bottom corner of the shape, and wrinkles that occur in the opposite corner (Figure 6.a). The “weave pattern heterogeneity” can be attributed to the severe stresses undergone by the fabric in this area of the preform due to the effect of blank-holder friction and the relatively small local radii. The presence of wrinkles on the useful area of the preform is more surprising. The shear angles (maximum 10° in left bottom corner and 28° in the right one) in these areas are lower than the theoretical locking angle (Figure 6.a). In addition, the yarns are subjected to high tension, due to the blank-holder pressure, which should prevent the occurrence of wrinkles. Although it is an interesting point, the full understanding of this phenomenon requires further investigations and is not within the scope of this study. All of these additional defects also occurred in the case of a monolayer preform oriented 30° (see Figure 6.b) and 60° in the same areas but not in the reference configuration (0°). On the other hand, the maximum shear angles measured on the oriented monolayer preforms remain substantially the same as those measured in the reference configuration (between 42 - 51°). It can then be concluded that whereas the shear angles remain in roughly the same range, the initial position of the fabric with respect to the punch has an effect on the type and number of defects when dealing with highly double curved shapes.

3.2.2. Two-layer forming: $0^\circ/\alpha^\circ$

Figure 7 shows the defect locations on the external and internal faces of the two-layer shape formed with configuration 2. This shape was produced with the external layer oriented 0° and the inner one 45° (denoted $0^\circ/45^\circ$). All the defect types observed on the previous preforms can be seen on the outer and inner plies but they are much more numerous than monolayer ones. As a result, the shape is far from being acceptable: the number of defects adversely influences the injection process and the mechanical properties of the final composite part. The inner ply oriented 45° shows more extensive and severe defects (Figure 7.a) than the 45° monolayer shape (Figure 6.a). The type and location of these defects remain substantially the same (Figure 8.a) but their magnitudes and their quantities are significantly

higher in the case of two-ply forming. The wrinkles, buckles and “weave pattern heterogeneity” that occurred in the bottom corners are larger than those of the monolayer preform and extend to the side faces. At the same time, the maximum shear angles remain relatively unchanged (between 42° and 50°). However, these plies are subjected to the same conditions (orientation, blank-holder pressure, etc.) except for the presence of the upper layer oriented at 0° . Considering that the latter exerts compaction on the inner ply, it should lead to a reduction in the amplitude and number of wrinkles, which is not the case. The increase in the number of defects is likely due to the effect of ply/ply friction that occurs for multilayer shaping and prevails over the compaction effect.

It has been shown that fabric/fabric friction behavior is the superposition of two phenomena (Figure 9) [29]. The first one is the yarn/yarn sliding friction that occurs between the yarns of the two plies. The second phenomenon is due to the shocks between the transverse overhanging yarns of each ply, at each period (or portion depending on the relative position of the plies) of the fabric unit cell. These shocks result in a high tangential reaction forces (denoted “F” on Figure 9) that lead to a considerable increase in the maximum friction values. The friction force then periodically exhibits peaks each time two “parallel” yarns of each sample encounter each other (Figure 10). The peak period can therefore be associated to the sample unit cell, as has been demonstrated in [29]. By inhibiting the relative motion of the adjacent plies, high friction forces therefore promote the occurrence of defects such as wrinkles and are responsible for the higher level of stresses in the fabric, which associated to the severe geometry of the shape (small radii), lead to fiber breakage (Figure 8.a).

Moreover, the shocks occurring between the yarns of the two plies also significantly impact the upper ply shearing and defects (Figure 7.b, Figure 8.b). This can be demonstrated by comparing the 0° ply on the 0° and $0^\circ/45^\circ$ stamping of the prismatic shape. In the case of the 0° monolayer, shear angles in the bottom corner are high (up to 55°) whereas no wrinkles occur in the useful areas. In contrast, on the $0^\circ/45^\circ$ configuration, defects (wrinkles and buckles) occur early during forming. In addition, shear angle values in the different areas also change (lower in the bottom corners, higher in the center of the front face, (Figure 8.b). The defects (buckles, wrinkles) of the 45° ply increase the surface irregularity, preventing the shearing of the upper 0° ply in the bottom corners. The higher shear angle values (62°) are then shifted toward the center of the front face.

3.2.3. Two-layer forming: $\alpha^\circ/0^\circ$

As indicated in section 2.3, two-ply forming was conducted, at first, by putting the oriented layer in the lower position to make the comparison as consistent as possible (Figure 2). Thus, the presence of the upper layer is the only difference when comparing the results of the oriented monolayer (α°) and the ($0^\circ/\alpha^\circ$) two-layer preforms. However, the measurements and observations on the layer of interest for multilayer forming require the demolding of the preform. This step may introduce variations in the defect amplitudes. To measure this influence, two-layer preforms were performed by putting the oriented ply on the top of the preform ($\alpha^\circ/0^\circ$).

Figure 11 shows a macroscopic external view of the ($45^\circ/0^\circ$) preform with the oriented ply placed in the upper position. The same defects in the same areas can be observed as noted previously in the configuration $0^\circ/45^\circ$ but with a higher amplitude. Table 1 illustrates a comparison among wrinkle dimensions measured on the 45° , $0^\circ/45^\circ$ and $45^\circ/0^\circ$ configurations. It can be observed that going from one ply to two plies significantly increases the wrinkle size (length, height, width) that was previously attributed to inter-ply friction. In addition, putting the oriented layer, that exhibits more defects, in the inner position results in less severe wrinkles. This effect is probably caused by the compaction exerted by the upper layer which flattens the wrinkles in the contour of the area where they occur. The pressure exerted by the upper ply on the lower one also explains the absence of wrinkles on the center of the front face when the oriented ply is the inner one (in the $0^\circ/45^\circ$ configuration, Figure 7.a), whereas Figure 11 and Figure 12 show that these wrinkles occur when the oriented ply is the upper one.

The same observation can be made concerning the buckles. The dimensions of the areas where the buckles occur are in the same range as those of wrinkles for the $0^\circ/45^\circ$ and $45^\circ/0^\circ$ cases (Figure 13.a). Remember that buckles are an out-of-plane bending at the yarn scale. This out-of-plane bending can reach a few millimeters as shown in Figure 13.b. When the ply is in the lower position, the compaction exerted by the upper one can lead to a significant decrease in this defect. This effect, if confirmed, can be one solution to reduce (or perhaps avoid) this kind of defect.

As a conclusion, the occurrence and the amplitude of the defects are related to the competition between two phenomena: the overhanging yarn shocks (due to inter-ply friction) which promote the defect and compaction which lowers them.

3.3. Inter-ply sliding

A previous study demonstrated that the fabric/fabric Coulomb friction coefficient for the interlock used here is sensitive to the relative orientation of the two samples [29]. It has also been shown that the average coefficient and the maximum tangential forces, due to shocks between transverse yarns of the two samples, are higher when the two samples are oriented at $0^\circ/0^\circ$ [29]. Therefore, friction should have a stronger effect on the occurrence of defects on the $0^\circ/0^\circ$ shapes, whereas, according to the results presented above, it is not the case. Furthermore, yarn shocks occur periodically in relation to the fabric meso-architecture, more precisely the unit-cell size, and the relative positioning of the yarn networks of the two samples. Nevertheless, as explained above, the friction effect comes from the relative sliding between the two plies. Consequently, if the two plies are perfectly superimposed and undergo the same strains, no relative sliding between the yarns of each ply occurs and then no friction effect is noticed. Even if, in a real forming test, two plies cannot be perfectly superimposed, a very small shift or misalignment between the two plies results in a very small relative sliding between them. No friction effect was noticed in this case. In the light of these observations, the following more accurate definition of

an acceptable sliding can be given. If the inter-ply sliding is significantly smaller than the unit-cell size, then the number of yarn/yarn shocks is too small to induce noticeable consequences on the forming result. This condition should be the case for the $0^\circ/0^\circ$ shapes. To assess this, inter-ply sliding was measured as indicated in section 2.3 along the lines (A to G) shown on Figure 2 and the results presented on Figure 14.

For the $0^\circ/0^\circ$ configuration, the measured average value is approximatively 3 mm inside the useful area of the shape and a maximum of 5 mm in the non-useful areas. The two layers are not formed under exactly the same conditions because the global shape on which the second layer is formed includes the first layer which modifies the shape dimensions slightly. However, this slight change cannot explain the displacement values (some millimeters). They are in all likelihood due to the placement and measurement accuracy and to the possible displacement introduced by the demolding of the preform. The markers (diameter between 1 and 2 mm) are painted on yarns of 2 mm width, which gives a measurement accuracy of approximately ≈ 2 mm. These measurements confirm that the relative displacement exists (the two layers do not remain perfectly superimposed) but also that it is significantly smaller than the unit-cell size (8 mm). The inter-ply friction, therefore, has no effect on the final quality of the two-layer preforms with $0^\circ/0^\circ$ orientations.

In contrast, the relative inter-ply sliding occurring on the $(0^\circ/\alpha^\circ)$ and $(\alpha^\circ/0^\circ)$ preforms is significantly larger, and is promoted by the relative position between the yarn networks (weft and warp) and the punch. The measured sliding reaches more than 70 mm for the $30^\circ/0^\circ$ shape (Figure 14). This value is promoted by the complex shape and is higher than that measured on the double-dome geometry (≈ 15 mm) by Bel and al. [23]. In the useful areas of the part without defects, a weak inter-ply sliding that is often less than 8 mm was observed. These areas are represented by color lines on the photo in Figure 14 and their corresponding measurements by color circles on the graphs in Figure 14. These values are smaller than the unit cell length of the G1151[®].

The defect areas exhibit higher inter-ply sliding than non-defect areas. This observation is noticeable both for the useful zones (which are the prism faces as far as Figure 14 is concerned) which are located from 0 to 300 mm from the shape center and for the non-useful zones. Considering the sliding distance along lines A and G, only one value exceeds the fabric unit cell length. It is located at the end of the layer (coordinate of 500 mm) where a wrinkle occurs. These observations confirm that the local relative sliding between yarns of the two layers is crucial for the occurrence and size of defects. Considering now the sliding distance along the lines (C, D and E), the inter-ply displacement increases earlier than the one along the other lines (A, G) and as a result, defects occur. The largest inter-ply sliding values were measured on the front face (line D). Along this line, a maximum inter-ply sliding of 72 mm was reached in the non-useful zone and a maximum inter-ply sliding of 33 mm was reached in the useful zone of the shape. According to the criteria previously proposed, the presence of wrinkles is unsurprising because the relative displacements in both cases represent four (on the useful zone) to nine (on the non-useful zone) times the unit cell length of the fabric.

It can be concluded that friction between plies can have a noticeable effect on the quality of the preform when inter-ply sliding is high. The fabric/fabric friction signal is periodic. The signal peaks represent shocks between overhanging yarns depending on the meso-architecture and on the relative

position between the two plies. The maximum values of the friction forces can therefore be reached in finite areas of the fabric only if the relative sliding is significantly greater than the unit-cell length. That is why even if the amplitude of the friction peaks is smaller in the case of the oriented layers, the finite sliding between the layers resulting from their relative orientation induces a much stronger friction effect.

4. Conclusion

This experimental work considered the effect of inter-ply friction on the occurrence of defects for multilayered composite shaping. Forming tests were performed on single-layer and multilayer shapes with different orientations. The results show that the initial position of the fabric with respect to the punch can have a major effect on the type and number of defects when working with highly double curved shapes. Despite the small shear angles and the high blank-holder pressure, wrinkles also occur for oriented monolayers.

Many of the defects and their location are generally the same for multilayered and single-ply shapes. However, the magnitude of each defect and the extent of the affected areas were significantly higher in the case of multilayered shapes. Additional defects, such as fiber breakage, were also observed in the same areas when forming several layers.

The measurements and observations conducted in this study highlight the effect of ply/ply friction caused by the relative sliding between layers on the defects and their occurrence. This effect has been related to a previous study on fabric/fabric friction [29] because it is due to the shock phenomenon occurring between the transverse overhanging yarns of each ply, at each period of the unit cell. This phenomenon hampers inter-ply relative sliding and intra-ply yarn movements (shear for instance), and generates high tangential forces with respect to the tension exerted on the yarns by the blank-holder pressure. It follows that this obstacle will promote the onset of wrinkles. However, its physical origin implies that this effect is significant only when the inter-ply sliding is larger than the unit cell length and leads to many shocks in a finite area of the fabric. In addition, when the oriented layers submitted to more defects are placed at the inner position of the lay-up, the compaction exerted by the outer plies leads to a slight decrease in the size of defects but not to their disappearance.

References

1. S. Hivet G., Allaoui S., Soulat D. Wendling A. Chatel, Analysis of woven reinforcement preforming using an experimental approach. Proceeding of the 17th International Conference on Composite Materials, Edinburgh, UK, July, 2009.
2. K. Vanclooster, S. Lomov, and I. Verpoest Simulation of multi-layered composites forming. International Journal of Material Forming, 2010; 3:695–698.
3. R.H.W. ten Thije, R. Akkerman, and J. Huétink. Large deformation simulation of anisotropic material using an updated lagrangian finite element method. Computer Methods in Applied Mechanics and Engineering, 2007; 196(33-34):3141–3150.

4. N. Hamila and P. Boisse, A meso macro three node finite element for draping of textile composite performs. *Applied Composite Materials*, 2007; 14:235–250.
5. J. Launay, G. Hivet, A.V. Duong, and P. Boisse, Experimental analysis of the influence of tensions on in plane shear behaviour of woven composite reinforcements. *Composites Science and Technology*, 2008; 68(2):506–515.
6. E. de Bilbao, G. Soulat, D. Launay, J. Hivet, A. Gasser, Experimental study of bending behaviour of reinforcements. *Experimental Mechanics*, 2010; 50(3):333–351.
7. G. Hivet and A.V. Duong, A contribution to the analysis of the intrinsic shear behavior of fabrics. *Journal of Composite Materials*, 2010; 45(6) 695–716.
8. P. Badel, E. Vidal-Sallé, P. Boisse, Computational determination of in-plane shear mechanical behaviour of textile composite reinforcements. *Computational Materials Science*, 2007; 40(4):439–448.
9. K.A. Fetfatsidis, D. Jauffrès, J.A. Sherwood, and J. Chen, Characterization of the tool/fabric and fabric/fabric friction for woven-fabric composites during the thermostamping process. *International Journal of Forming*, 2013; 6(2), 209-221.
10. K.A. Fetfatsidis, L. M. Gamache, J. L. Gorczyca, James A. Sherwood, D. Jauffrès, and J. Chen, Design of an apparatus for measuring tool/fabric and fabric/fabric friction of woven-fabric composites during the thermostamping process, *International Journal of Forming*, 2013; 6(1), 1-11.
11. D. Soulat , S. Allaoui, S. Chatel, Experimental device for the performing step of the RTM process. *International Journal of Material Forming*, 2009; 2 (1):181-184.
12. S. Allaoui, P. Boisse, S. Chatel, N. Hamila, G. Hivet, D. Soulat, E. Vidal-Salle, Experimental and numerical analyses of textile reinforcement forming of a tetrahedral shape. *Composite Part A*, 2011; 42(6):612-622.
13. Thomas Gereke, Oliver Döbrich, Matthias Hübner, Chokri Cherif, Experimental and computational composite textile reinforcement forming: A review. *Composite part A*, 2013; 46:1-10.
14. Vanclooster K, Lomov SV, Verpoest I., Experimental validation of forming simulations of fabric reinforced polymers using an unsymmetrical mould configuration. *Composites A*, 2009; 40(4):530–539.
15. R.H.W. ten Thije, R. Akkerman, A multi-layer triangular membrane finite element for the forming simulation of laminated composites. *Composites: Part A*, 2009; 40:739–753.
16. P. Harrison, R. Gomes, N. Curado-Correia, Press forming a 0/90 cross-ply advanced thermoplastic composite using the double-dome benchmark geometry. *Composites: Part A*, 2013; 54:56–69.
17. Peng Wang, Nahiène Hamila, Philippe Boisse, Thermoforming simulation of multilayer composites with continuous fibres and thermoplastic matrix. *Composites: Part B*, 2013; 52:127–136.
18. Qianqian Chen, Philippe Boisse, Chung Hae Park, Abdelghani Saouab, Joël Bréard, Intra/inter-ply shear behaviors of continuous fiber reinforced thermoplastic composites in thermoforming processes. *Composite Structures*, 2011; 93:1692–1703.

19. K. Vanclooster, S.V. Lomov and I. Verpoest, Simulation of multi-layered composites forming. *Int J Mater Form*, 2010; 3(1):695– 698.
20. Boisse P, Hamila N, Vidal-Sallé E, Dumont F, Simulation of wrinkling during textile composite reinforcement forming. Influence of tensile, in-plane shear and bending stiffnesses. *Compos Sci Tech*, 2011; 71(5):683–692.
21. Willems A, Lomov SV, Verpoest I, Vandepitte D, Harrison P, Yu WR. Forming simulation of a thermoplastic commingled woven textile on a double dome. *Int J Mater Form*, 2008; Suppl 1: 965–968.
22. N. Hamila, P. Boisse, F. Sabourin, and M. Brunet. A semi-discrete shell finite element for textile composite reinforcement forming simulation. *International Journal for Numerical Methods in Engineering*, 2009; 79(12):1443–1466.
23. Bel, N. Hamila, P. Boisse, F. Dumont, Finite element model for NCF composite reinforcement preforming: Importance of inter-ply sliding. *Composites: Part A*, 2012; 43:2269–2277.
24. Nahiene Hamila, Philippe Boisse, Simulations of textile composite reinforcement draping using a new semi-discrete three node finite element. *Composites: Part B*, 2008; 39:999–1010.
25. Nahiene Hamila, Philippe Boisse, A Meso–Macro Three Node Finite Element for Draping of Textile Composite Preforms. *Appl Compos Mater*, 2007; 14:235-250.
26. M.A. Khan, T. Mabrouki, E. Vidal-Sallé, P. Boisse, Numerical and experimental analyses of woven composite reinforcement forming using a hypoelastic behaviour. Application to the double dome Benchmark. *Journal of Materials Processing Technology*, 2010; 210(2):378–388
27. S. Allaoui, G. Hivet, D. Soulat, A. Wendling, P. Ouagne and S. Chatel, Experimental preforming of highly double curved shapes with a case corner using an interlock reinforcement. *International Journal of Material Forming*, 2014; 7(2):155-165.
28. G. Hivet, S. Allaoui, B.T. CAM, P. Ouagne, D. Soulat, Design and potentiality of an apparatus for measuring yarn/yarn and dry fabric/dry fabric friction. *Experimental Mechanics*, 2012; 52 (8):1123-1136.
29. S. Allaoui, G. Hivet, A. Wendling, P. Ouagne, Soulat, Influence of the dry woven fabrics meso-structure on fabric/fabric contact behavior. *Journal of Composite Materials*, 2012; 46(6):627-639.
30. S.V. Lomov and I. Verpoest. Model of shear of woven fabric and parametric description of shear resistance of glass woven reinforcements. *Composites Science and Technology*, 2006; 66(7-8):919–933.
31. P., Abdiwi, F., Guo, Z., Potluri, P., and Yu, W.R., Characterising the shear-tension coupling and wrinkling behaviour of woven engineering fabrics. *Composites Part A: Applied Science and Manufacturing*, 2012; 43 (6), 903-914.

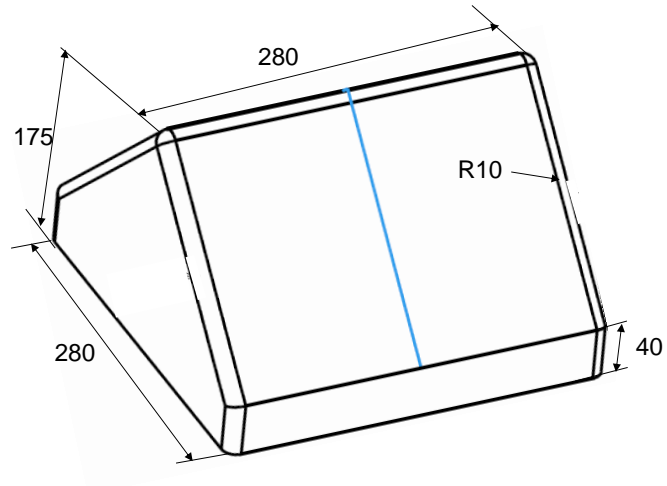


Figure 1: Prismatic shape used for this study (all dimensions are in mm).

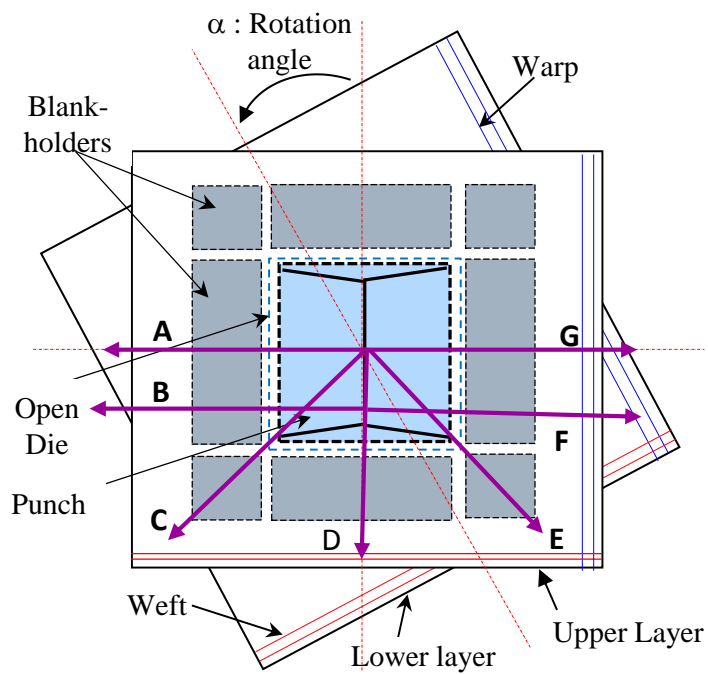


Figure 2: Initial positioning of the fabric for two-layer forming.

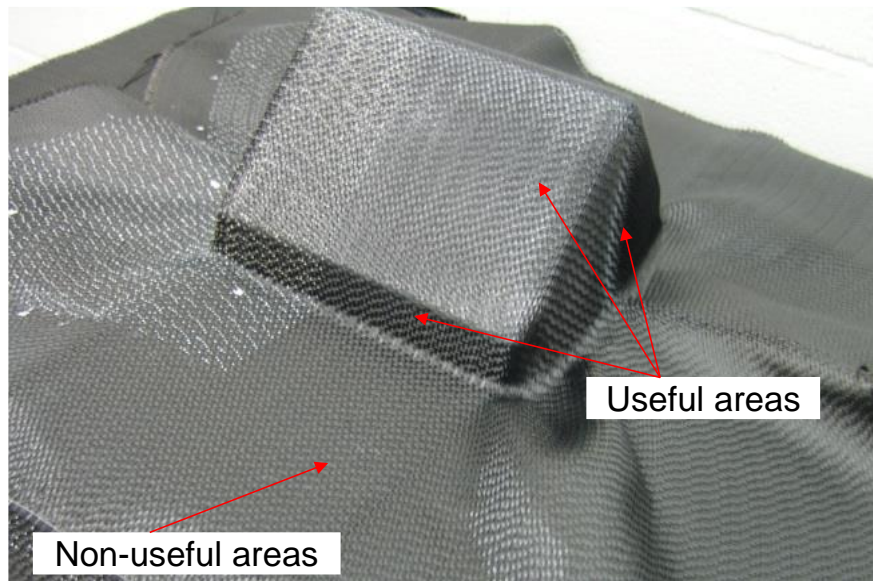


Figure 3: View of the prismatic shape for two-layer forming with configuration 1 ($0^{\circ}/0^{\circ}$)

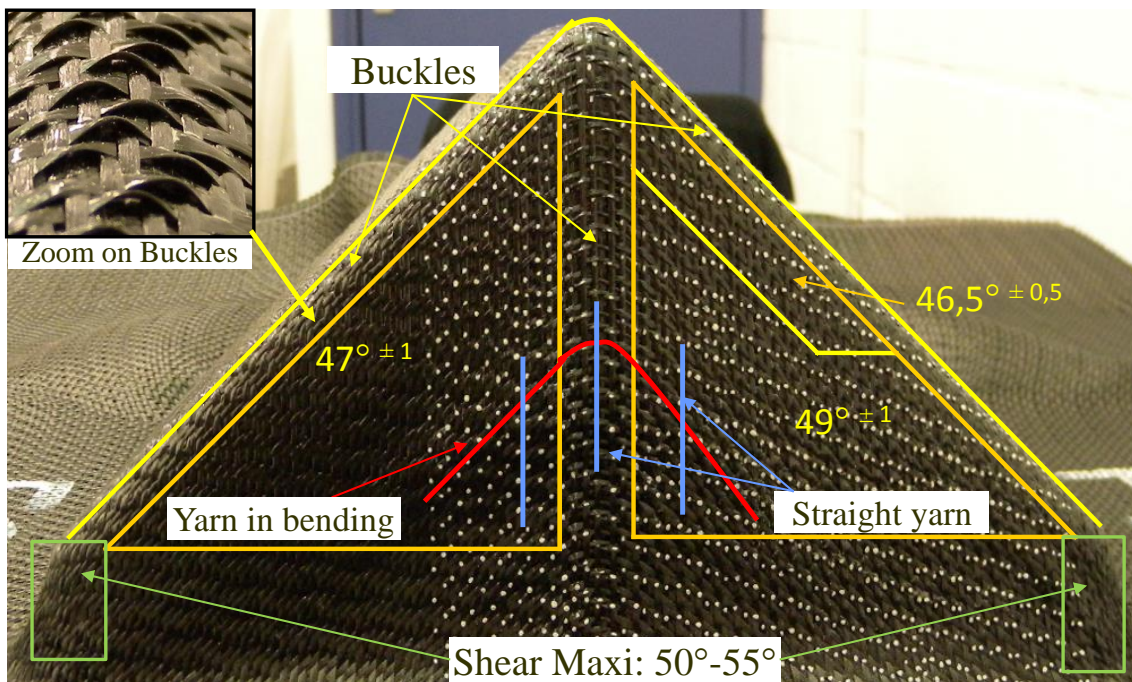


Figure 4: Shear angles and defects on the front face of the prismatic shape of two-layer forming with configuration 1 ($0^{\circ}/0^{\circ}$).

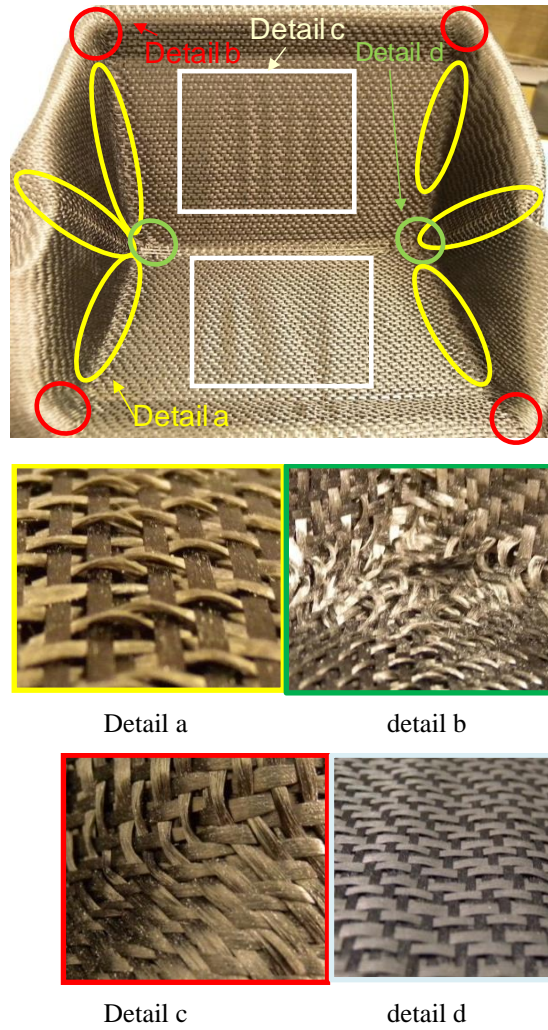
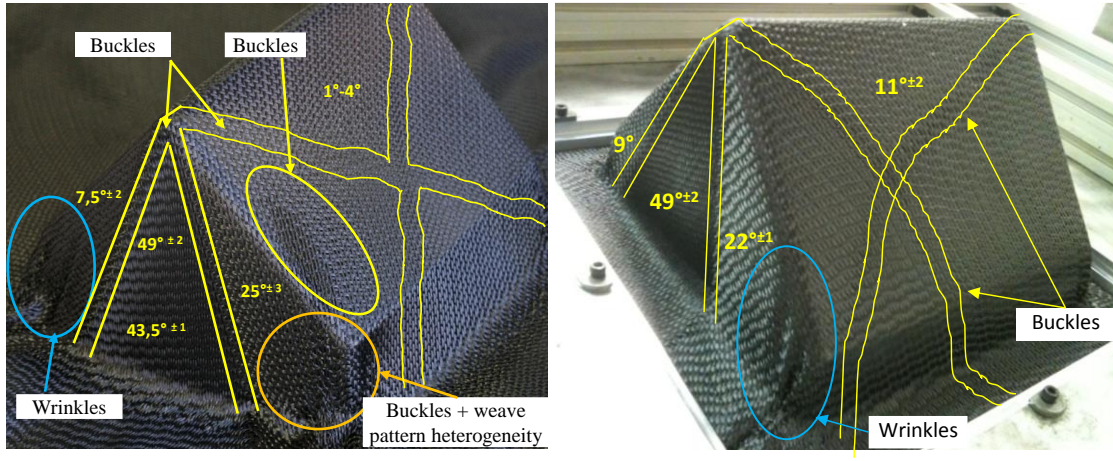


Figure 5: View of the inner faces of the two-layer prismatic shape formed with configuration 1 ($0^\circ/0^\circ$).

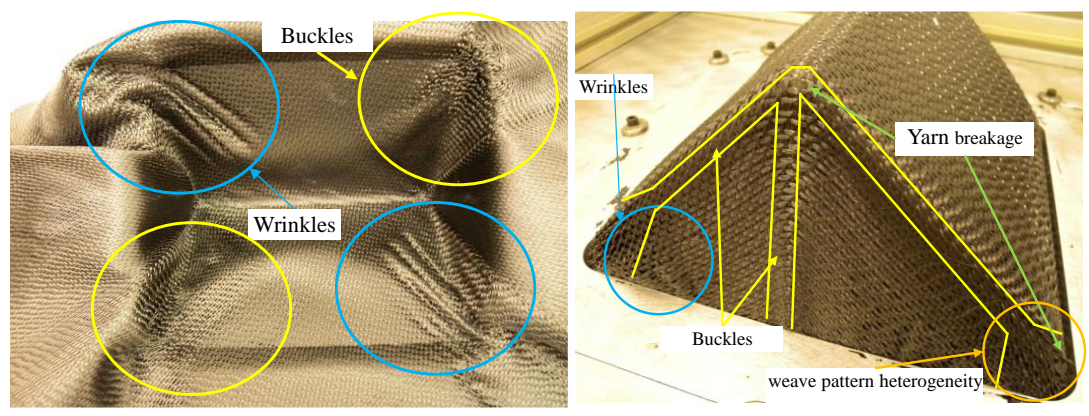
Detail a: buckles; detail b: fiber breakage; detail c: buckles + weave pattern heterogeneity; detail d: wrinkles.



(a) Monolayer oriented at 45°

(b) Monolayer oriented at 30°

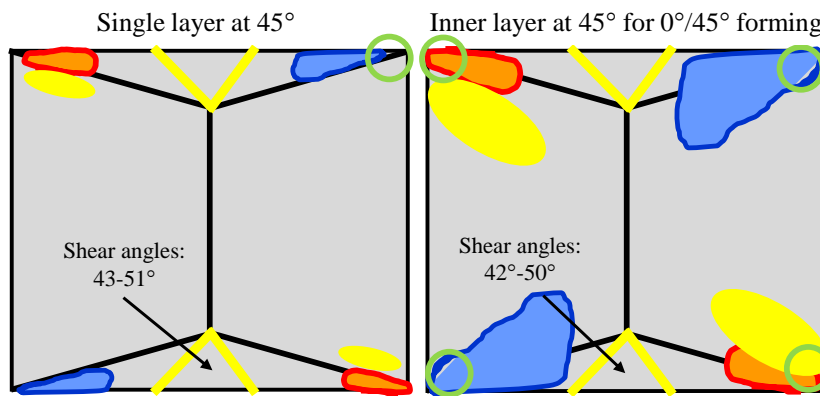
Figure 6: View of the monolayer (α°) prismatic shape formed with configuration 2.



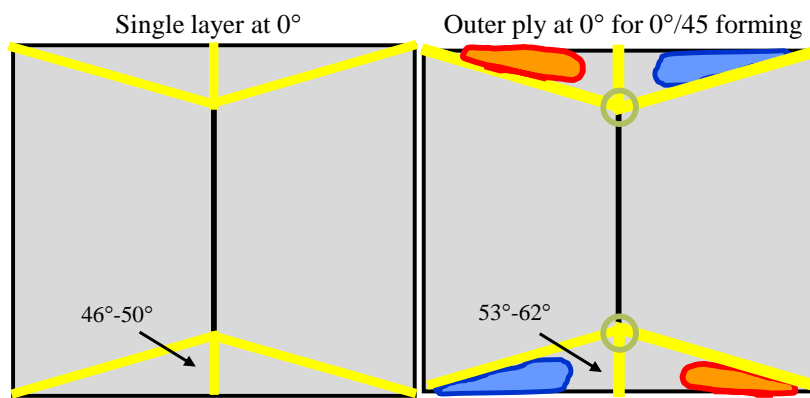
(a) Inner ply (45°)

(b) Outer ply (0°)

Figure 7: View of the two-ply (0°/45°) prismatic shape formed with configuration 2



(a) Layers oriented at $\alpha=45^\circ$



(b) Layers oriented at $\alpha=0^\circ$

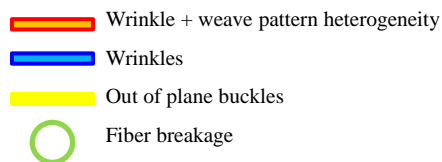


Figure 8: Comparison of defects between the two-layer of $0^\circ/45^\circ$ configuration and monolayers at 0° and 45° configurations.

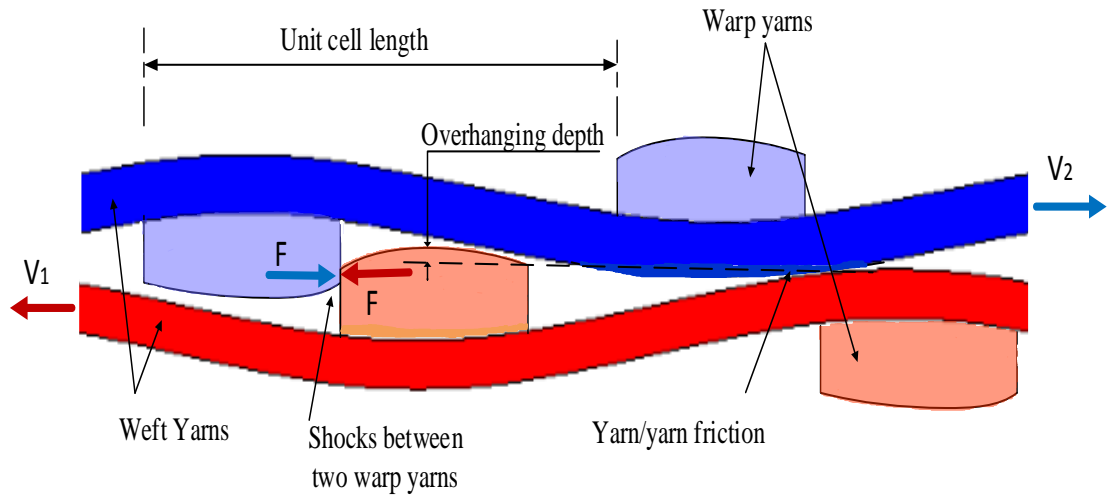


Figure 9: Phenomena occurring during fabric/fabric friction: yarn/yarn friction and shock phenomenon caused by overhanging yarns [27].

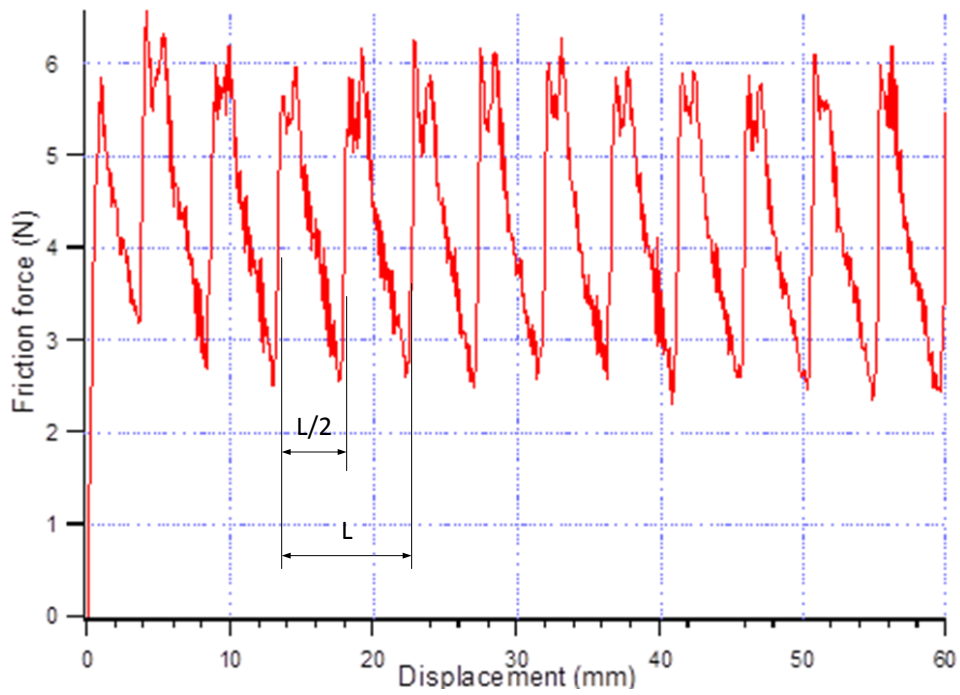


Figure 10: Evolution of tangential load during fabric/fabric friction test of G1151[®] reinforcement (L: unit cell length).

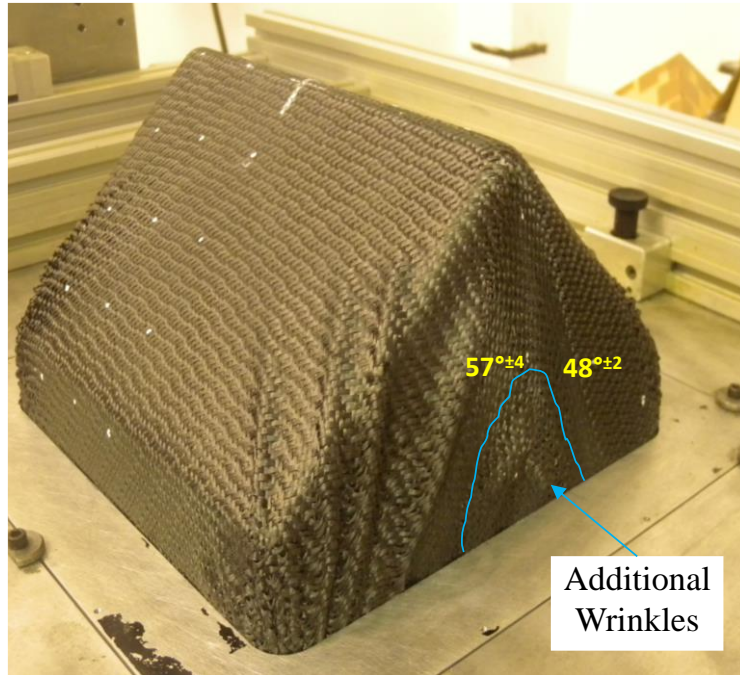


Figure 11: External view of the preforms performed with two-layer ($45^\circ/0^\circ$): inner layer at 0° and outer layer at 45° .

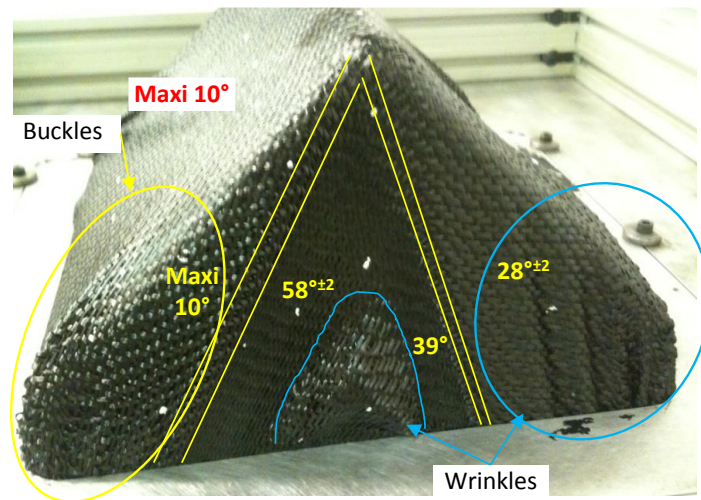


Figure 12: Two-layer preform in the $30^\circ/0^\circ$ configuration. (upper layer at 30°)



(a) Buckles and wrinkles on the side face

(b) Buckles at the bottom corner

Figure 13: Quantification of defects on the outer layer (45°) of the two-layer preform ($45^\circ/0^\circ$).

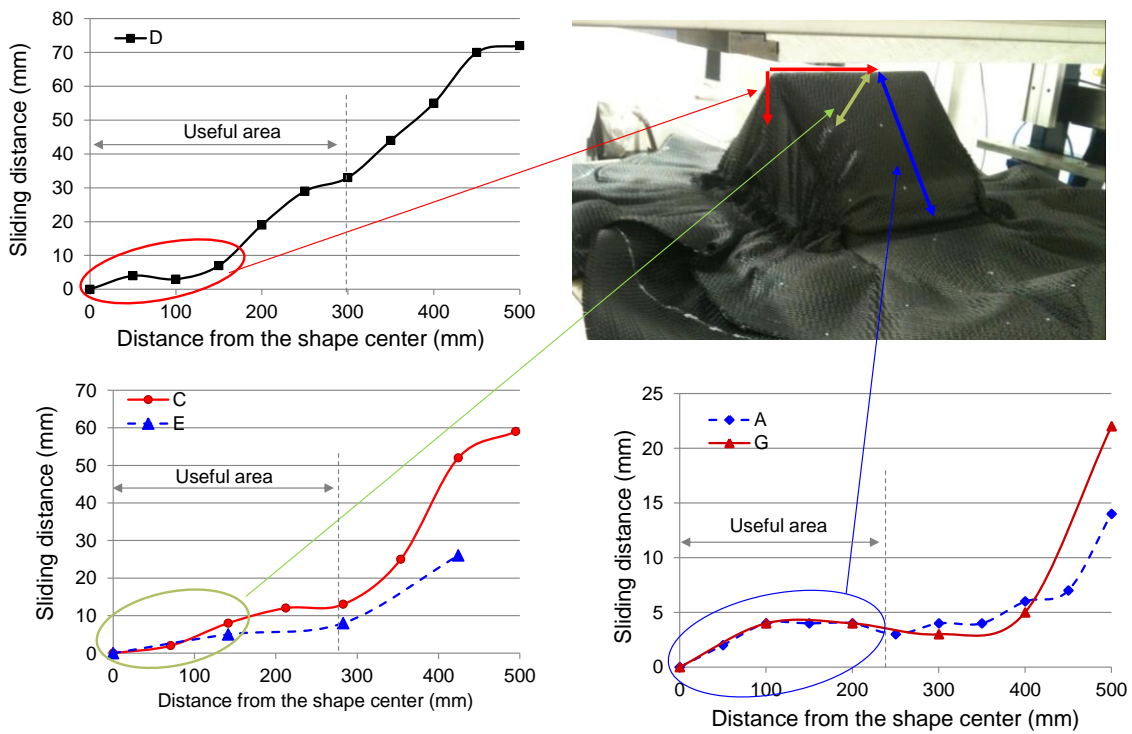


Figure 14: Inter-ply sliding measurements for the two-layer forming ($30^\circ/0^\circ$). The photo represents the final preform. The lines A, C, D, E and G (represented by different colors) are those where the markers were placed on the preform in order to measure the relative sliding between layers (see figure 2). The graphs represent the measured relative sliding.